Design of optical micromachines for use in biologically relevant environments

Andrew, Philippa Kate; Fan, Daniel; Raudsepp, Allan; Lofroth, Matthew; Staufer, Urs; Williams, Martin A.K.; Avci, Ebubekir

DOI
10.1109/AIM43001.2020.9158816

Publication date
2020

Document Version
Final published version

Published in
Proceedings of the IEEE/ASME International Conference on Advanced Intelligent Mechatronics, AIM 2020

2020 IEEE/ASME International Conference on
Advanced Intelligent Mechatronics (AIM), Boston, USA
(Virtual Conference), July 6-9, 2020

Design of Optical Micromachines for Use in Biologically Relevant Environments*

Philippa-Kate Andrew[1], Daniel Fan[2], Allan Raudsepp[3], Matthew Lofroth[1], Urs Staufer[2], Martin A. K. Williams[3,4] and Ebubekir Avci[1,4]

***Abstract*— Advances in nanofabrication over the past twenty years have enabled the creation and use of ever-more interesting and useful micromachines. Optical micromachines are a particularly attractive subset of these for researchers in biological and soft-matter sciences, due to their potential to aid in optical tweezer studies of laser-sensitive samples. However, the development of multi-component micromachines is made difficult due to the dominance of surface forces at this scale, which is made all the more relevant in the high-salt concentrations used for biological studies. This study concerns the design of simple, first-class lever micromachines for use in environments with different salt concentrations, in an attempt to provide a guideline for design requirements of functional optical micromachines for use in physiological conditions.**

I. INTRODUCTION

The pervasiveness of adhesion forces at the micro and nanoscale has presented a challenge to researchers interested in micromanipulation. In the area of optical micromanipulation, these adhesion forces hinder the actuation of multi-component optical microrobots, due to the low forces provided by optical tweezers (10^{-14} – 10^{-10} Newtons) [1]. Despite the restriction on force magnitude, the associated resolution of displacement and force makes optical manipulation an attractive option for life-science research [2]–[5]. However, optical tweezers also present serious drawbacks, namely the potential for damaging biological objects under study [6], [7]. While the exact mechanisms for this damage are not agreed upon, studies have identified several possible pathways including localised heating [8], [9], photogenerated free radicals [10] and photobleaching [11]. Optical micromachines present an exciting opportunity for reducing damage to biological subjects, as well as the potential for extending optical tweezers to new uses [12]. However, the propensity for surface forces to dominate has meant that researchers are faced with challenges when it comes to designing multi-component micromachines that work reliably. While optical tweezers have been used to perform micromanipulation in air [13], traditionally, optical micromanipulation is performed in a liquid medium. Trapping objects submerged in a liquid allows researchers to neglect inertial terms in analysis of an object's movement in a trap [14], and reduces electrostatic and capillary forces. The reduction of these forces theoretically reduces the adhesion forces between surfaces, which is vitally important for the successful actuation of multi-component micromanipulators. This is demonstrated in the literature in the cases of levers [15], micromanipulators that transform an in-plane translation to an out of plane rotation [16], and micro-gears [17]. In these studies, trapping took place in milliQ water- ultra pure water deionised until it has a resisitivity of 18.2 MΩcm- and a surfactant was added to lower adhesion forces between components, improving the chance of success. However, in order to use optical micromanipulators as tools for research in the life sciences, rather than as research curiosities, micromanipulators must be functional in cellular conditions. Hence, rather than milliQ water, the micromanipulators need to be tested in biologically relevant salt concentrations. This is important as the ionic strength of the surrounding medium has been demonstrated to affect the properties of biological samples; for instance the elasticity of DNA is affected by the amount of salt in the medium [18]. Salts screen repulsive electrostatic interactions between objects due to reduction of the Debye length [19], thus, adhesion between parts of multi-component micromanipulators becomes more of an issue as salt increases. This work aims to determine the geometry required for levers with equal-length arms to function in tris-buffered saline (TBS), which has a molarity of 150 mMol sodium chloride (NaCl), and contains 45 mMol of Tris and hydrochloric acid in order to maintain a slightly alkaline pH of 7.5. The use of salty buffers such as TBS, has two functions in biological studies, with one being to maintain an environment with biological ionic strength, and the other being to inhibit undesirable enzymatic functions, so that biological molecules and processes can be observed without undesirable changes taking place during the experiment. This selectivity has allowed researchers to directly observe enzyme behaviour in highly controlled conditions [20]. These kinds of interactions cannot be studied in milliQ water, and so optical micromachines that are functional in different mediums are required.

*This work was supported by the Marsden Fund Council from New Zealand Government funding, managed by Royal Society Te Aparangi (MAU1714)

[1]Philippa-Kate Andrew, Matthew Lofroth and Ebubekir Avci are with the Department of Mechanical and Electrical Engineering, Massey University, Palmerston North 4442, New Zealand. e.avci@massey.ac.nz

[2]Daniel Fan and Urs Staufer are with the Department of Precision and Micro Engineering, Technische Universiteit Delft, 2600 AA Delft, The Netherlands.

[3]Allan Raudsepp and Martin A.K. Williams are with the School of Fundamental Sciences, Massey University, Palmerston North 4442, New Zealand.

[4]Martin A.K. Williams and Ebubekir Avci are affiliated with the MacDiarmid Institute for Advanced Materials and Nanotechnology, Wellington 6140, New Zealand.

978-1-7281-6794-7/20/$31.00 ©2020 IEEE

Previous works regarding the problem of adhesion for microrobotics have identified surface forces as problems for pick-and-place tasks [21], [22], as attractive forces between the micromachine and target object make precise placement and release difficult. However, in this study the focus is on the effects of attractive forces on the functionality of multi-part micromachines. In the case of multi-part micromachines, non-contact attractive forces between parts are of particular concern, as the parts must be separate, and in the case of pin-jointed structures, must retain their axis of rotation. In this work, structural variations of a 1:1 first-class microlever were tested in a series of different TBS solutions, ranging in strength from 1% to 50% TBS. The performance of different designs was then evaluated with respect to overall success rate, and the way in which the levers moved. This paper covers the theory associated with screened electrostatic interactions briefly, before detailing the design and manufacture of optical micromachines and discussing the results of trialling the levers in different concentrations of Tris-buffered saline solutions. As an extension, anti-digoxigenin coated microbeads were attached to the microlevers, to demonstrate their potential use as a tool for biological studies.

II. Methods

A. Theory

Traditional models for attractive force between micro-objects in liquids are based on DLVO theory [23], which was developed to describe the stability of aqueous dispersions. This theory describes the stability of systems as being determined by two groups of forces, the van der Waals and electrostatic forces, which govern the dispersion and aggregation of particles in the system. The total contribution to the forces that exist between particles can then be expressed as:

$$F_{DLVO} = F_{vdW} + F_{el} \tag{1}$$

Where F_{vdW} is the contribution provided by van der Waals interactions between the objects, and F_{el} is the contribution from electrostatic forces. As the attractive van der Waals forces are significant only at very small displacements, the repulsive electrostatic interactions generally dominate the interaction. However, as levers move the distance between parts may become small enough for van der Waals forces to temporarily overcome electrostatic repulsion and lead to contact and adhesion between parts. This effect is facilitated further by lower electrostatic repulsion when the Debye length shortens.

Electrostatic interactions between particles in an electrolyte solution are caused by the surface charging of the particles, due to adsorption of ions within the solution and resultant ionising reactions with the material of the particle [24]. Both parts of the micromachine are made from the same material, and immersed in the same fluid, and so it is assumed that the charge on the surfaces will be similar, and consequently repulsive. The expression for this interaction

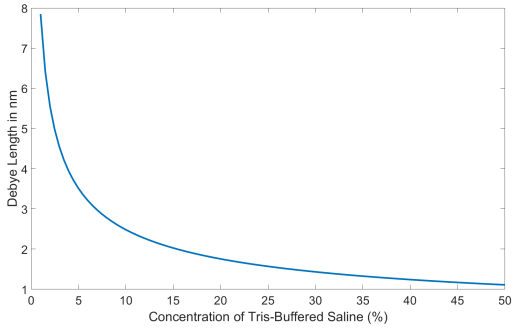

Fig. 1. The dependence of the Debye length on the concentration of TBS, according to (3).

relies on the Debye length [19], as can be seen in (2), which gives the electrostatic force between two identical spheres, positioned a distance x apart, where $x < 2R$. In this equation R is the diameter of the particles, Z is the surface charge, κ^{-1} is the Debye length, ϵ_0 is the permittivity of free space, ϵ_r is the relative permittivity and e_c is the elementary charge.

$$F(x) = (e_c^2 Z^2/(8\pi\epsilon_0\epsilon_r R^3))\kappa^{-1}e^{-\kappa x} \tag{2}$$

The Debye length, which is given by κ^{-1}, is in turn influenced by the concentration of salt in the solution, as shown in (3). In this empirical expression the Debye length is taken to be completely dependent on the concentration of cations, n_c, and anions, n_s in the bulk.

$$\kappa^{-1} = 0.304/\sqrt[4]{n_s n_c} \tag{3}$$

Given that adding salt reduces the Debye length, consequently reducing the stabilising electrostatic repulsion, there is good theoretical basis to investigate the effect that geometry has on the functionality of multi-component micromachines in high-salt environments. While this equation is for the case of two spheres, it provides a clear illustration of how electrostatic forces in aqueous solutions are affected by the addition of salt, as well as an indication of the dependence of the force on object separation.

Seven different concentrations of TBS were used in this study, and it was approached from a simplistic perspective where the shortening of the Debye length would lead to a higher chance of component adhesion. Therefore, the dependence of successful lever turning on salt concentration should produce a results graph with a similar shape to the one illustrating the change in Debye length with increasing TBS concentration (Fig. 1).

B. Design and Manufacturing

This work was done as part of a project geared towards developing micromachines for use in biological experiments using optical tweezers. Therefore, levers were designed with this objective in mind. This led to the concept of a 1:1 first class lever, which can be used to transfer force over its fixed central axis to the target. Levers have been successfully utilised in the literature for force-multiplication [15], [25],

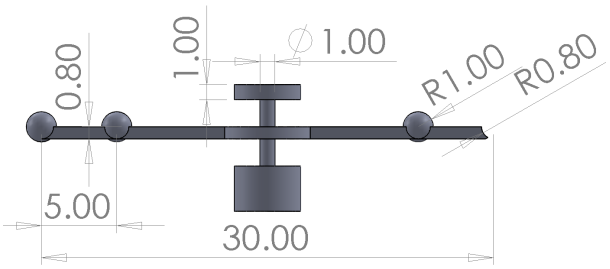

Fig. 2. The basic design was a first-class lever, with equal length arms. Three spherical features are positioned as trapping handles, and a pocket is positioned at the end of the lever. All measurements are in micrometres.

which implies that the force applied on one side of the equal-armed lever can be transferred over the joint to be applied elsewhere. The levers all featured three spherical trapping handles and a pocket on one end (Fig. 2). This pocket is intended for the optional attachment of a functionalised microbead which can then be used to probe biological subjects, or for direct attachment to a target object such as a red blood cell. The spheres located part-way along the lever arms allow for the use of two balanced optical traps to rotate the levers, rather than just using one trap on the end of the lever, although this is also an option for equal force transfer. From this basic first design several different iterations were produced, with this paper focusing on variations of this design featuring three different kinds of support structures, varying overlapping surface area and slight changes in part separation. Five variations of the design were trialled in this work, with 20 levers in each batch, and the features of these designs are detailed in Fig. 3 and Table I, where the features of the different designs can be compared. The horizontal separation between the pin and the lever arm was kept at 1.6 μm for all designs in order to minimise contact area with the pin. Additionally, initial trials of lever functionality in milliQ water showed that this dimension allowed for centred rotation around the pin, while smaller separation distances led to increased likelihood of stiction.

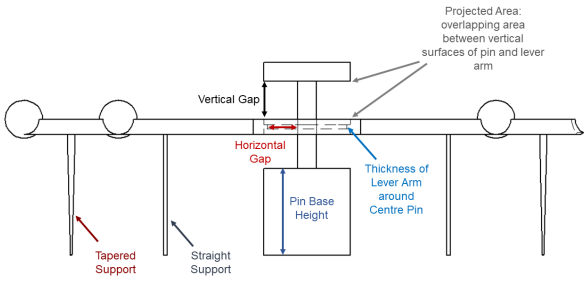

Fig. 3. Five variations of the basic 1:1 lever were used in this paper. Two of these designs featured no supporting structures, while the other three were supported using either straight or tapered supports. Additionally, centre-pin height, vertical gap size and lever arm thickness varied between designs.

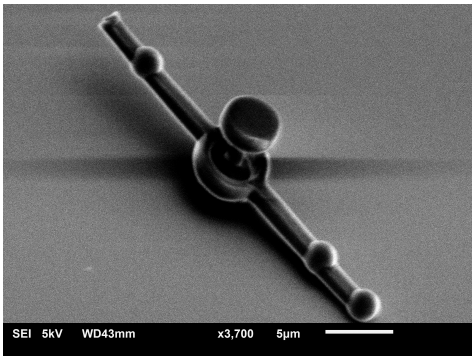

Fig. 4. The "No Supports" type lever under SEM.

Levers were manufactured using the Nanoscribe GmbH Photonic Professional, a laser-based 3D printer capable of producing objects with 50 nm resolution using the technique of two-photon absorption polymerisation (TPAP) [26]. The photoresist used was Nanoscribe's proprietary IP-L 780 resist. Levers were designed using SolidWorks and printed from .stl files, similar to conventional macro-scale 3D printing. The choice of laser power for printing was made following several trials, and it was found that 13 mW consistently produced levers with the resolution required, with minimal instances of printing errors caused by resin bubbling. An SEM image of one of the levers can be seen in Fig. 4.

C. Experimental

Levers were kept on the original substrate that they were printed on, and a borosilicate microprobe with a tip-radius of approximately 1 μm was used to detach support material in dry condition, and turn the levers to ensure functionality. Following this initial step, the levers were turned 360° in milliQ water, which took place to ensure all levers were in a freely moving state. Levers were kept attached to the substrate by the bases of the centre pins in order to provide a stable rotation point. A lever was considered ready for optical trapping when it rotated in response to the drag force of the microprobe, as this is approximately the same magnitude as the force supplied by optical tweezers, in the high tens of pico-Newtons.

Following preparation using the microprobe, samples were taken to the optical trapping apparatus. Holographic optical tweezers were used for this work, and the setup consisted of a Nikon Eclipse TE2000 inverted microscope, Arryx Holographic Optical Tweezers and Basler Ace ac2040-uc CMOS and Andor Neo sCMOS cameras for imaging, all isolated from vibration. The HOT was comprised of a 2W 1064 nm infrared laser and a Boulder Nonlinear Systems phase-only spatial light modulator (SLM); with a 1.2 numerical aperture, 60x magnification Nikon plan APO water-immersion lens used to focus the beam. A 1.5x secondary objective was used to further increase the image magnification to 90x. The Arryx Labryx software was used to control power to the laser, while the Red Tweezers software developed by

TABLE I

FEATURES OF LEVERS USED IN THIS STUDY.

Sample	Support Style	Overlapping Area (Vertical Projection)	Lever Arm Thickness (around centre pin)	Horizontal Gap	Vertical Gap	Pin Base Height
Straight Supports	Straight	1.35 μm^2	0.8 μm	1.6 μm	2.0 μm	3.0 μm
Conical Supports, Low Contact	Tapered	1.35 μm^2	0.2 μm	1.6 μm	1.8 μm	3.0 μm
Conical Supports, Low Contact 2	Tapered	1.41 μm^2	0.2 μm	1.6 μm	2.1 μm	4.8 μm
No Supports	No Support	1.35 μm^2	0.8 μm	1.6 μm	1.8 μm	3.0 μm
No Supports, High Pin	No Support	1.35 μm^2	0.8 μm	1.6 μm	2.0 μm	4.6 μm

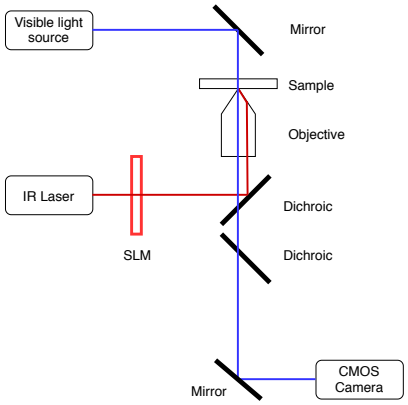

Fig. 5. The optical trapping set-up used for the work. This diagram was previously published in [12].

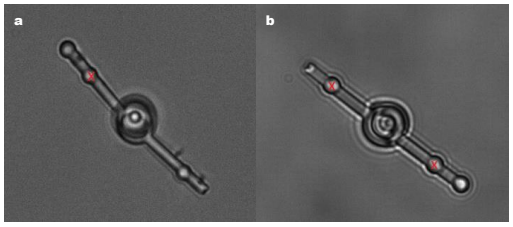

Fig. 6. Trapping was performed using a holographic optical trap, placed on one of the "inner" trapping handles, as shown here with the red "x" in (a). If a full turn was not possible in this configuration, or if the lever moved out of focus due to the unbalanced force, then two traps were used, as shown in (b).

Bowman et al. was used to position optical traps [27]. A diagram of the setup is shown in Fig. 5.

Trapping was performed at maximum power, and the trap was positioned as shown in Fig. 6a for a stable trap. The trap was then moved in order to rotate the lever a full 360°, which was regarded as a success. If the lever did not make the full 360° turn with one trap, or if the lever was pulled out of focus, then two traps would be used, as shown in Fig. 6b. The first experiment with each set of levers was trapping performed in high purity milliQ water. Trapping was performed with the laser passing through the substrate that the levers were printed on, and the samples were not sealed, due to the need to change the trapping liquid, and to manipulate the levers with the borosilicate microprobe. This meant that evaporation of the medium was an issue, but liquid was added to the substrate as required during the experiment, with 80 μl added at the start of the microprobe step, and a further 40 μl added before optical trapping. While open-substrate trapping is not common, it is useful in circumstances when contact manipulation of micro-objects is required in between optical trapping [28]. After trapping was conducted in milliQ water, the liquid was wicked away using a Kim Wipe. This was performed with the aid of the Olympus IX71 inverted microscope, at a magnification of 16x, in order to ensure that the levers were not accidentally removed in the process and that the liquid was properly removed. Optical trapping was carried out in six different concentrations of TBS, as well as in milliQ water, which provided the baseline results for each group of levers. The order of experiments is shown in Table II. The decision was made to only use concentrations of up to 50% TBS due to the likelihood of excess salt being present on the substrate due to the method of adding and removing the solution throughout the experiment. This means that the actual concentration of TBS that remained on the sample could be close to double the expected amount. However, the lowest amounts that could possibly be present have been quoted here; i.e. the concentration of TBS added to the sample in each experiment.

The Andor Neo sCMOS camera was used to video the trapping experiments, collecting video at a frame rate of 100fps. These videos were then analysed using ImageJ [29] for information about how the levers responded to the traps.

III. RESULTS AND DISCUSSION

The first subject of interest for this work was the success rate of lever operation. This was defined as the percentage of levers out of a batch that turned at every concentration of TBS used. Levers were then defined as either successfully rotating; exhibiting a limited response to the optical trap; or

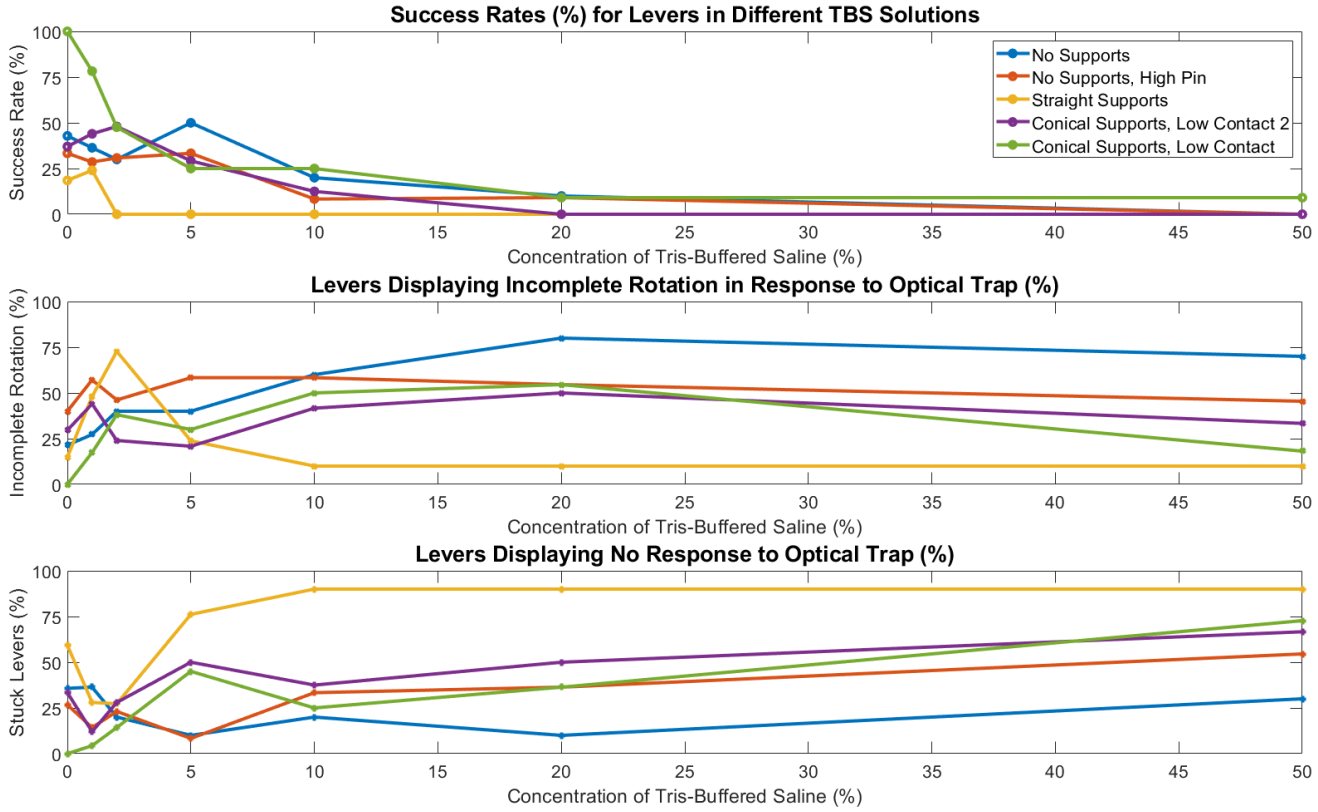

Fig. 7. Lever performance was simply grouped into three categories: successful, multiple 360° turns (top); response to the optical trap but no full turns, where out-of-plane movement and limited rotation are counted (middle); and stuck levers (bottom).

TABLE II
TRIS-BUFFERED SALINE CONCENTRATIONS USED FOR TRAPPING

Experiment Run	TBS Concentration (%)
Run 1	0 (milliQ water)
Run 2	1
Run 3	2
Run 4	5
Run 5	10
Run 6	20
Run 7	50

having no response to the trap. These results can be seen in Fig. 7. Only one group of levers demonstrated successful 360° turning in each medium. This group was the Conical Support, Low Contact (CSLC) sample, where levers had a 1.6 μm separation between the inside of the lever arm and the centre pin, a 1.8 μm separation between the lever arm and the base of the centre pin and tapered supports which served to decrease the surface area in contact with the substrate, while also maintaining the vertical separation between lever arm and pin and reducing out of plane motion. The next-best performing designs were the unsupported ones: labelled No Support (NS) and No Support, High Pin (NSHP). There was little difference between these two designs, indicating that the effect of increasing vertical separation between lever arm and pin and between the lever and the substrate had minimal impact. The worst performing group of levers was the Straight Supports (SS) sample. This was unsurprising as this group featured both the thickest lever arm; with respect to projected thickness onto the centre pin; and supports with more surface area in contact with the substrate when compared to the tapered kind.

Initially, it had been expected that the performance of Conical Supports, Low Contact 2 (CSLC2) would be very similar, or potentially better than CSLC. However, while the thin ridges added to the centre pin increased the gap between the thin ridge on the lever arm and the centre pin, these ridges also led to the likelihood of the lever arm "cupping" the centre pin when they moved off-centre, or if the levers settled downwards. Freely-moving, and hence trappable, levers move off-centre due to thermal fluctuations, and so this became a major source of poor performance for this lever group. The relevant dimensions can be seen in Fig. 8. Theoretically, the presence of the supports should have stopped this "cupping" from happening, but the sample-preparation using the microprobe can be damaging, leading to bending and deformation of supports. The thinness of the supports also means that they bend in response to even very low forces, as can be seen in the two video stills in Fig. 9, where the supports flex against the turning of the lever. Additionally, the slightly larger projected vertical area would also have contributed to increased attractive force between the two components. While the levers without supports

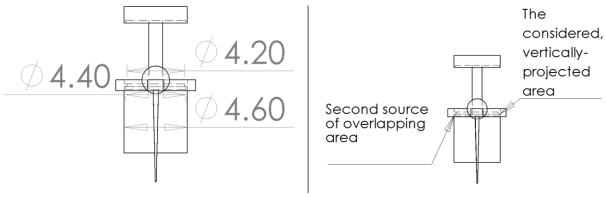

Fig. 8. The ridges added to the centre-pin served to keep overlapping area small, and increase vertical separation. However, the size of the outer cut-out on the lever arm was the same diameter as the outside of the pin, meaning that "cupping" of the centre pin during settling would actually increase the contact area between parts.

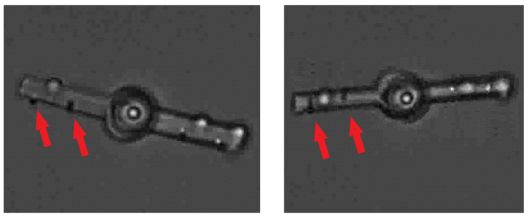

Fig. 9. In this case it is possible to see the support structures flexing against the lever turning. Due to the strength of adhesion between the substrate and the supports, a full turn was impossible, but the supports were flexible enough to allow slight twisting and rotation around the axis. The red arrows point to two of the supports, showing a slight change in position and angle.

performed relatively well, out-of-plane rotation increased severely compared to the supported levers when using a single trap. Therefore, using two traps and rotating them around the axis became the method of choice. The difference in out-of-plane motion when using one trap versus using two can be seen in the set of stills shown in Fig. 10. While all lever groups largely complied with the predicted effects of increased TBS concentration, the results from the CSLC group matched the shape of the Debye curve very closely. This could be due to the fact that the supports and geometry of the lever arm enabled relatively consistent projected area and separation throughout the experiment,

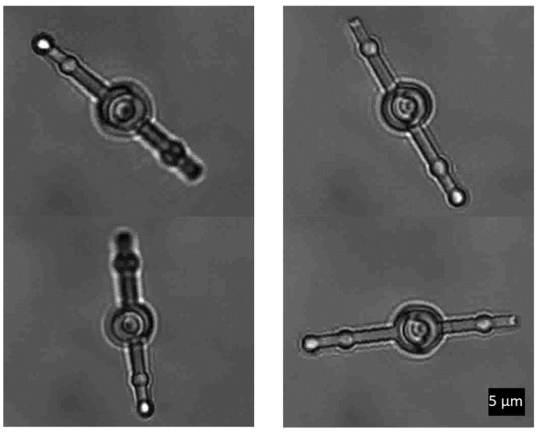

Fig. 10. Unsupported levers required two traps to ensure planar rotation. In these stills from the trapping videos for NS levers in milliQ water the difference between trapping using a single trap (left) and symmetric rotating traps (right) can be clearly seen.

whereas levers with higher contact area ceased to move at much lower concentrations (SS, CSLC2) and the supportless levers demonstrated more out-of-plane motion, and so less consistent part separation. This demonstrates the inherent difficulty in predicting behaviour of optical micromachines, which has motivated studies by other researchers, including one regarding pose estimation from video, due to the difficulty calculating this from conventional forward dynamics [30]. The lack of predictability could be put down to small changes in surface roughness and individual differences between levers in a batch. The relatively small sample size of 20 levers in each sample also means that these results are statistically limited, and it is possible that larger sample sizes and more gradually varying concentrations of TBS would result in graphs that better followed the expected shape. Additionally, while the TBS solutions were kept chilled before use, and experiments with each sample took place over the course of a single day, colonisation of samples by bacteria, and build up of dust was an issue that could have introduced differences in sample environment. Future experiments could take place in a sealed chamber. However, different samples would need to be used due to the inability to change the fluid or prepare samples using the microprobe, which would introduce further variation in samples.

Grouping all non-360° responses to optical trapping as "limited response" means that a true comparison of lever performance is difficult to gauge. Therefore, the non-360° responses for each sample were compared, as well as the mechanisms which caused sticking. From Fig. 7, it is clear that the supported styles have more instances of "no rotation" responses to the optical traps. This is due to the fact that the reason for loss of functionality for these levers tended to be the support structures sticking to the substrate. This was in direct contrast with the unsupported levers, which tended to start to stick around the axle, and tended to more gradually lose the ability to turn, which is potentially due to progressively stronger attraction to the axle as the Debye length decreases.

A separate experiment was performed with a batch of ten levers of the NS style. This involved slowly adding TBS to the sample to increase the concentration of the solution used as the trapping medium, while using the optical tweezers to guide 2.12 μm diameter anti-digoxigenin coated microbeads into the pockets at the ends of the levers. Ten attempts were made at each concentration, with no successful adhesion of the bead with the lever observed until the concentration reached 5% TBS, when all ten attempts were successful. This is significant as the Debye length is predicted to have dramatically shortened at 5% TBS compared to lower concentrations, and this is also where four out of five samples showed a sizeable decrease in success rate. A before-and-after of the attachment process can be seen in Fig. 11. The use of these beads in DNA-stretching protocols makes the ability to securely attach them to the levers an important step forward in demonstrating the potential for optical machine-assisted biological studies.

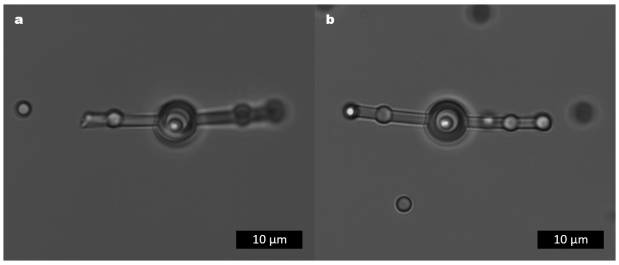

Fig. 11. Microbeads could be successfully attached to functional levers at 5% TBS. Before attachment (a) and after (b).

IV. Conclusions

The experiments performed demonstrate that geometry of optical micromachines is vitally important for functionality when the ionic strength of the trapping medium is increased from minimal levels. The data gained from the comparison of these levers show that small, nanoscale differences in design make a large difference in functionality, and that taking a considered approach to this may save many research hours of trial and error. The introduction of support structures as a method for reducing out-of-plane motion is one that has not been seen elsewhere in the literature, and the results from this study demonstrate that this is not only viable, but that this design out-performs more conventional unsupported designs, when other design features are also carefully considered. Additionally, the successful attachment of microbeads at 5% TBS corroborates the other findings regarding the effects of increased molarity on Debye length. The results from this work, which are congruent with a very basic model of electrostatic attraction between surfaces, will serve as a baseline for further work in modelling micromachine behaviour in different environments.

References

[1] C.-H. Lien, M.-T. Wei, T.-Y. Tseng, C.-D. Lee, C. Wang, T.-F. Wang, H. D. Ou-Yang, and A. Chiou, "Probing the dynamic differential stiffness of dsdna interacting with reca in the enthalpic regime," *Opt. Express*, vol. 17, no. 22, pp. 20 376–20 385, Oct 2009.

[2] A. Keloth, O. Anderson, D. Risbridger, and L. Paterson, "Single cell isolation using optical tweezers," *Micromachines*, vol. 9, no. 9, 8 2018.

[3] A. van der Horst and N. R. Forde, "Calibration of dynamic holographic optical tweezers for force measurements on biomaterials," *Opt. Express*, vol. 16, no. 25, pp. 20 987–21 003, Dec 2008.

[4] M. Capitanio and F. S. Pavone, "Interrogating biology with force: Single molecule high-resolution measurements with optical tweezers," *Biophysical Journal*, vol. 105, no. 6, pp. 1293 – 1303, 2013.

[5] M. Cruceanu, A. G. Stephen, P. J. Beuning, R. J. Gorelick, R. J. Fisher, and M. C. Williams, "Single dna molecule stretching measures the activity of chemicals that target the hiv-1 nucleocapsid protein," *Analytical Biochemistry*, vol. 358, pp. 159–170, 2006.

[6] M. B. Rasmussen, L. B. Oddershede, and H. Siegumfieldt, "Optical tweezers cause physiological damage to escherichia coli and listeria bacteria," *Applied and Environmental Microbiology*, vol. 74, pp. 2441–2446, 2008.

[7] K. König, "Laser tweezers are sources of two-photon effects," in *Multiphoton Microscopy and Fluorescence Lifetime ImagingApplications in Biology and Medicine*, K. König, Ed. Berlin, Germany: Walter de Gruyter GmbH, 2018, ch. 9, pp. 177–188.

[8] A. Chowdhury, D. Waghmare, R. Dasgupta, and S. K. Majumder, "Red blood cell membrane damage by light-induced thermal gradient under optical trap," *Journal of Biophotonics*, vol. 11, no. 8, p. e201700222, 2018.

[9] I. Krasnikov, A. Seteikin, and I. Bernhardt, "Thermal processes in red blood cells exposed to infrared laser tweezers (λ = 1064 nm)," *Journal of Biophotonics*, vol. 4, no. 3, pp. 206–212, 2011.

[10] M. P. Landry, P. M. McCall, Z. Qi, and Y. R. Chemla, "Characterization of photoactivated singlet oxygen damage in single-molecule optical trap experiments," *Biophysical journal*, vol. 97, pp. 2128–2136, 2009.

[11] S. Ayano, Y. Wakamoto, S. Yamashita, and K. Yasuda, "Quantitative measurement of damage caused by 1064-nm wavelength optical trapping of escherichia coli cells using on-chip single cell cultivation system," *Biochemical and Biophysical Research Communications*, vol. 350, no. 3, pp. 678 – 684, 2006.

[12] P.-K. Andrew, M. A. K. Williams, and E. Avci, "Optical micromachines for biological studies," *Micromachines*, vol. 11, no. 2, 2020.

[13] R. Omori, T. Kobayashi, and A. Suzuki, "Observation of a single-beam gradient-force optical trap for dielectric particles in air," *Opt. Lett.*, vol. 22, no. 11, pp. 816–818, Jun 1997.

[14] M. D. Summers, D. R. Burnham, and D. McGloin, "Trapping solid aerosols with optical tweezers: A comparison between gas and liquid phase optical traps," *Opt. Express*, vol. 16, no. 11, pp. 7739–7747, May 2008.

[15] C.-L. Lin, Y.-H. Lee, C.-T. Lin, Y.-J. Liu, J.-L. Hwang, T.-T. Chung, and P. L. Baldeck, "Multiplying optical tweezers force using a microlever," *Opt. Express*, vol. 19, no. 21, pp. 20 604–20 609, Oct 2011.

[16] E. Avci, M. Grammatikopoulou, and G.-Z. Yang, "Laser-printing and 3d optical-control of untethered microrobots," *Advanced Optical Materials*, vol. 5, no. 19, p. 1700031, 2017.

[17] S. Maruo, K. Ikuta, and H. Korogi, "Force-controllable, optically driven micromachines fabricated by single-step two-photon microstereolithography," *Journal of Microelectromechanical Systems*, vol. 12, no. 5, pp. 533–539, Oct 2003.

[18] C. G. Baumann, S. B. Smith, V. A. Bloomfield, and C. Bustamante, "Ionic effects on the elasticity of single dna molecules," *Proceedings of the National Academy of Sciences*, vol. 94, no. 12, pp. 6185–6190, 1997.

[19] M. R. Griffiths, A. Raudsepp, K. M. McGrath, and M. A. K. Williams, "Measuring the interaction between a pair of emulsion droplets using dual-trap optical tweezers," *RSC Adv.*, vol. 6, pp. 14 538–14 546, 2016.

[20] F. M. Fazal, D. J. Koslover, B. F. Luisi, and S. M. Block, "Direct observation of processive exoribonuclease motion using optical tweezers," *Proceedings of the National Academy of Sciences*, vol. 112, no. 49, pp. 15 101–15 106, 2015.

[21] M. Gauthier, S. Régnier, P. Rougeot, and N. Chaillet, "Analysis of forces for micromanipulations in dry and liquid media," *Journal of Micromechatronics*, vol. 3, pp. 389–413, 2006.

[22] R. S. Fearing, "Survey of sticking effects for micro parts handling," *Proceedings 1995 IEEE/RSJ International Conference on Intelligent Robots and Systems. Human Robot Interaction and Cooperative Robots*, vol. 2, pp. 212–217, 1995.

[23] B. V. Derjaguin, N. V. Churaev, and V. M. Muller, *The Derjaguin—Landau—Verwey—Overbeek (DLVO) Theory of Stability of Lyophobic Colloids*. Boston, MA: Springer US, 1987, pp. 293–310.

[24] S. H. Behrens and D. G. Grier, "The charge of glass and silica surfaces," *The Journal of Chemical Physics*, vol. 115, no. 14, pp. 6716–6721, 2001.

[25] Y. J. Jeong, T. W. Lim, Y. Son, D.-Y. Yang, H.-J. Kong, and K.-S. Lee, "Proportional enlargement of movement by using an optically driven multi-link system with an elastic joint," *Opt. Express*, vol. 18, no. 13, pp. 13 745–13 753, Jun 2010.

[26] S. Maruo, O. Nakamura, and S. Kawata, "Three-dimensional microfabrication with two-photon-absorbed photopolymerization," *Opt. Lett.*, vol. 22, no. 2, pp. 132–134, Jan 1997.

[27] R. Bowman, G. Gibson, A. Linnenberger, D. Phillips, J. Grieve, D. Carberry, S. Serati, M. Miles, and M. Padgett, ""red tweezers": Fast, customisable hologram generation for optical tweezers," *Computer Physics Communications*, vol. 185, no. 1, pp. 268–273, 1 2014.

[28] I. Shishkin, H. Markovich, Y. Roichman, and P. Ginzburg, "Auxiliary optomechanical tools for 3d cell manipulation," *Micromachines*, vol. 11, no. 1, 2020.

[29] C. A. Schneider, W. S. Rasband, and K. W. Eliceiri, "Nih image to imagej: 25 years of image analysis," *Nature Methods*, vol. 9, pp. 671–675, 2012.

[30] M. Grammatikopoulou and G. Yang, "Three-dimensional pose estimation of optically transparent microrobots," *IEEE Robotics and Automation Letters*, vol. 5, no. 1, pp. 72–79, Jan 2020.